Chemical Physics Letters 830 (2023) 140774

Contents lists available at ScienceDirect

Chemical Physics Letters

journal homepage: www.elsevier.com/locate/cplett

Benzodithiophene-based Acceptor-Donor-Acceptor-type compounds for highly efficient organic photovoltaic cells

R. Kacimi [a,*], E. Tanıs [b], A. Azaid [a], Y. Khaddam [a], M. Raftani [a], S. Sarfaraz [c], L. Bejjit [d], M. Bouachrine [a,e,*]

[a] CMC-Molecular Chemistry and Natural Substances Laboratory, Faculty of Sciences, University Moulay Ismail, Meknes, Morocco
[b] Department of Electrical Electronics Engineering, Kırsehir Ahi Evran University, 40100 Kırşehir, Turkey
[c] Department of Chemistry, COMSATS University Islamabad, Abbottabad Campus, KP 22060, Pakistan
[d] MEM, LASMAR Laboratory, University Moulay Ismail, Meknes, Morocco
[e] EST Khenifra, Sultane Moulay Slimane University, Khenifra, Morocco

ARTICLE INFO

Keywords:
Indandione
Benzodithiophene
DFT
Organic solar cells (OSCs)

ABSTRACT

In this study, the structural, optical and electronic properties of a conjugated A-D-A compound based on indandione and benzobitiophene, which is widely used in the production of organic solar cells, were theoretically calculated using different functionals of the Density Functional Theory (DFT) method. For this purpose, different parameters such as frontier molecular orbital (FMO), which is called the highest occupied molecular orbital HOMO and the lowest unoccupied molecular orbital LUMO, energy gap E_{gap} (HOMO-LUMO), the density of states (DOS), the absorption maximum λ_{max}, excitation energy E_{ex} and transition density matrix (TDM) were calculated. In addition, reduced density gradient (RDG) and open circuit voltages V_{OC} were simulated to evaluate hole-electron localization. According to the results obtained from this study, the investigated compound exhibits significant visual absorption and interesting electron transport properties due to its hard-flat structures. The open circuit voltage (V_{OC}) of compounds with BTPF acceptors is 1.45 V. This study has shown that BTPF compound has great potential for integration into solar cells as an electron donor material and has provided evidence that the investigated material may be a potential photovoltaic material candidate.

1. Introduction

Organic photovoltaic (OPV) cells are one of the most potential next-generation photovoltaic technologies to capture pure, renewable and unlimited solar energy due to their advantages such as low weight, wide absorption range, thermal stability and flexibility compared to inorganic silicon-based solar cells with high thermal stability. Compared to inorganic silicon-based solar cells with limited applications due to their inflated costs, flexible designs and low efficiencies, OPV cells have advantages such as thermal stability, flexibility, mechanical compliance and ease of preparation. In the last few decades, OPV cells have attracted global attention as photoactive materials in academic and commercial sectors. Additionally, there are numerous publications in the valuable literature that theoretical construct and test various active layer molecules for use in solar cell applications. After bridging adjustments, discovered many donor compounds for extremely efficient solar cells. For effective solar cell applications, constructed and theoretical studied C-shape molecules. The various acceptor compounds based on benzothiadiazole units for high-performance organic solar cells were also tested [1–5]. Many scientific studies have been conducted on the design of new organic materials. One of the main objectives of these studies is the design of new organic materials with interesting structural, optical and electronic properties. By taking advantage of the benefits of the great efforts made to increase the power conversion efficiencies of OPV cells, PCEs have been improved up to 15–19% [6,7].

Due to their remarkable power conversion efficiencies, small-molecular donors based on benzodithiophene have lately gained appeal in organic solar cells (OPVs)[8]. There is currently a limited selection of organic electron acceptor materials. It is primarily caused by molecules becoming unstable once they carry an electron, electron-accepting semiconductors need to have the following qualities in order to be employed in photovoltaic devices: strong chemical and thermal stability and high electron mobility[9]. One of the most popular electron acceptor materials for organic electronics is the molecule

* Corresponding authors.
E-mail addresses: r.kacimi@edu.umi.ac.ma, kacimirachid71@gmail.com (R. Kacimi).

https://doi.org/10.1016/j.cplett.2023.140774
Received 28 May 2023; Received in revised form 27 July 2023; Accepted 17 August 2023
Available online 20 August 2023

indandione[10,11]. An indandione-type core unit has recently drawn attention as an effective electron acceptor unit in the continuation of organic moieties because to its numerous modification sites and strong electron-withdrawing abilities[12]. By creating tiny organic molecules with various acceptor–donor-acceptor (A-D-A)[13–15] combinations and examining the impact of these combinations on optoelectronic and photovoltaic capabilities, it is possible to make major structural alterations to the indandione-type core unit[16–20]. In the current study, we used the polymer benzodithiophene as an electron-donating example because it has better solubility in most nonaromatic solvents, a simple planar structure, strong UV–visible absorptions, and is directly bordered by end capping groups that are used as electron acceptors to create OPV cells. Based on the indandione moiety straightforward production and potential for chemical modification, an electron-accepting moiety was chosen. Inspired by the results of the recent investigations of indandione and benzodithiophene, with the aim of investigating the structural, optical, and electronic properties of a molecule designed and synthesized by Ling et al [21]. The selection of this compound was based on the simplicity of the synthesis and the chemical modification possibility of the ring acceptors moieties, which has a direct impact on most of the materials properties, including the HOMO, E_{gap}, photoluminescence spectra, etc. Just too briefly, the remainder of the manuscript will refer to this compound as BTPF. The newly emerging high-efficiency BTPF which has a central fused ring ((benzobitiophene) core), we modified its alkyl side chains and the addition of an acceptor group at the exterior to enhance its electron-withdrawing ability (Schema 1).

The purpose of this article is to determine the structural, optoelectronic and photovoltaic properties (E_{HOMO}, E_{LUMO}, E_{gap}, λ_{max}…) of the BTPF molecule using Density Functional Theory (DFT) and Time-Dependent Density Functional Theory (TD-DFT) and to select the most appropriate method by comparing the results obtained with experimental results in the literature. In addition to these, the potential of BTPF compound as a donor molecule was tested by using fullerene compound PCBM, and fullerene derivative PC61BM as acceptors [22].

2. Results and discussion

2.1. Computational details

This theoretical study was carried out in order to study the structural, electronic, optical, and photovoltaic properties of the compound BTPF. All calculations in this study were completed using the Gaussian 09 program [23] in the gas phase. The inputs and for the visualization of results were made using Gauss view 6.0 [24]. In order to validate the functional method adopted in the experimental results, the density functional theory (DFT) was used with the different sets of functional bases B3LYP[25], MPW1PW91 [26], WB97XD [27], and CAM-B3LYP [28]. 6-31G(d,p) [29–33], 6–31 + G(d,p), 6-311G(d,p) and 6-311++G (d,p)[34,35] basis set were used for study the optoelectronic and geometrical properties (E_{HOMO}, E_{LUMO}, E_{gap}, λ_{max}…) of the BTPF. After several calculations and testing, the value of the gap energy of the molecule BTPF obtained by B3LYP with 6–31++G(d,p) basis set was in good agreement with close to the experimental. Thus, it was the best choice for the remaining calculations of compound BTPF. To get the values of the λ_{max} absorptions, oscillator strengths, and vertical electronic excitation spectra of BTPF we used the TD-DFT approach on the DFT/B3LYP/6-31G(d,p) [36], DFT/B3LYP/6–31 + G(d,p), DFT/B3LYP/6-311G(d,p), DFT/B3LYP/6-311++G(d,p) optimized structures [37]. We also used the TD-MPW1PW91/6-31G(d,p), and TD-CAM-B3LYP [38] methods the latter was used thanks to their ability to describe well the absorption properties of π-conjugated systems according to [39]. The functional which gave the value λ_{max} absorptions close to the experimental by TD-B3LYP at 6-311++G(d,p) basis set. The Density of State (DOS) spectra were plotted via PyMOlyze-1.1 [40], transition density matrix (TDM), Reduced Density Gradient (RDG) analyses were plotted with by Multiwfn [41], and drawn with the VMD version 1.9.1 [42]. The GaussSum software was used to interpret the nature of the transitions and estimate the percent contribution of the predominant transition [40].

2.2. Electronic properties

The Bandgap it a crucial factor for realistic electron mobility. Indeed, a molecule with a narrower band gap will have a higher charge mobility rate, hence the need for calculation, In order to have a general idea of the electronic properties of the studied compound [43]. The application of various DFT functions offers the opportunity to compare the experimental and theoretical values in order to choose the functional method that reflects well the correlation between the electrical properties of the BTPF obtained experimentally and those obtained theoretically.

The difference between experimental and theoretical results may be due to the fact that DFT calculations of BTPF compound were performed in the gas phase, where there is no interaction. The HOMO and LUMO energy levels and E_{gap} gap energy of the BTPF compound are tabulated in Table 1.

According to Table 1, the HOMO, LUMO and gap energies calculated by the B3LYP/6-31G(d,p), B3LYP/6-311G(d,p), B3LYP/6–31 + G(d,p), B3LYP/6-311++G(d,p), MPW1PW91/6-31G(d,p), MPW1PW91/6-311G(d,p), WB97XD/6-31G(d,p) and WB97XD/6-311G(d,p) methods are respectively (-5.61,-5.84, −5.92, −5.95, −5.85, −6.03, −7.17 and −7.34 eV), (-3.57, −3.81, −3.91, −3.95, −3.54, −3.74, −2.01 and −2.20 eV) and (2.04, 2.03, 2.01, 2.00, 2.31, 2.29, 5.16 and 5.14 eV). The results obtained with the B3LYP functional and the 6-311++G(d,p) basis set are found to be quite close to the experimental data (-5.68,-4.06

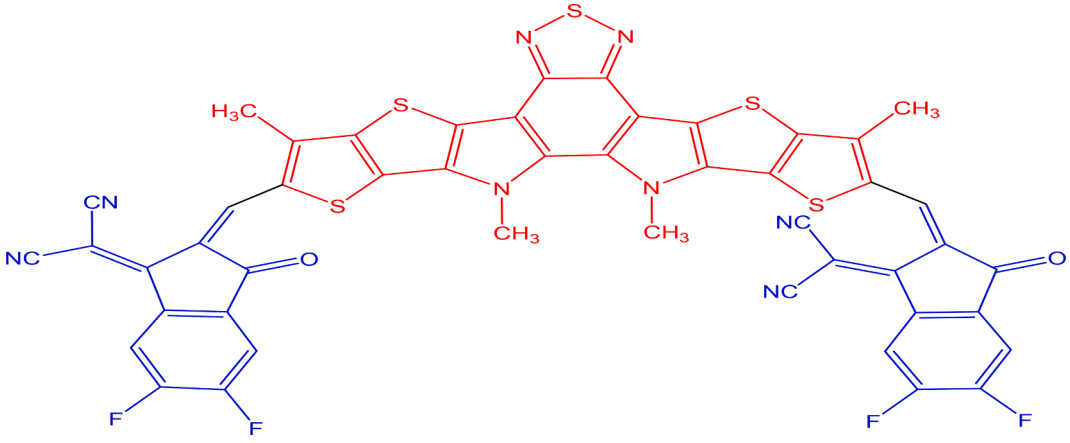

Schema 1. Chemical structure of BTPF compound.

Table 1
Calculated theoretical values of the HOMO and LUMO and energy gap E_{H-L} of the BTPF molecule in (eV) with different functional.

Methods	E_{HOMO}	E_{LUMO}	E_{gap}
B3LYP/6-31G(d,p)	−5.61	−3.57	2.04
B3LYP/6-311G(d,p)	−5.84	−3.81	2.03
B3LYP/6–31 + G(d,p)	−5.92	−3.91	2.01
B3LYP/6-311++G(d,p)	−5.95	−3.95	2.00
MPW1PW91/6-31G(d,p)	−5.85	−3.54	2.31
MPW1PW91/6-311G(d,p)	−6.03	−3.74	2.29
WB97XD/6-31G(d,p)	−7.17	−2.01	5.16
WB97XD/6-311G(d,p)	−7.34	−2.20	5.14
Exp[21].	−5.68	−4.06	1.62

and 1.62 eV). As a result, it can be concluded that the B3LYP functional with the 6-311++G (d,p) basis set is the most compatible with experimental data for describing the electrical properties of the chemical compound under investigation.

The results of the electronic properties obtained by the quantum method B3LYP/6-311++G(d,p) were confirmed by the calculation of the optical properties of the compound studied. We conducted several calculs by the quantum chemistry methods TD-DFT/B3LYP/6-31G(d,p), TD-DFT/B3LYP/6–31 + G(d,p), TD-DFT/B3LYP/6-311G(d,p), TD-DFT/B3LYP/6-311++G(d,p), TD-DFT/CAMB3LYP6-31G(d,p), and TD-DFT/MPW1PW91/6-31G(d,p). On the optimized geometries by each method in order to choose the best quantum method to describe the effects of excitation and electronic transition, the derived values of the E_{ex}, oscillator strengths (f), and λ_{max}.

According to Table 2, λ_{max} was calculated as (680.93, 693.93, 685.68, 695.72, 560.91 and 652.07 nm) for TD-DFT/B3LYP/6-31G(d, p), B3LYP/6–31 + G(d,p), B3LYP/6-311G(d,p), B3LYP/6-311++G(d,p), CAMB3LYP6-31G(d,p) and MPW1PW91/6-31G(d,p) functions, respectively. However, according to the experimental values stated in the literature [20], the optical absorption values of the BTPF compound are found in the wavelength range of 600–900 nm. It is understood from the results obtained with TD-B3LYP/6-311++G (d,p) that is closest to the result in the literature. The difference between the results is thought to be due to the calculations being performed in the gas phase These findings suggest that the absorption characteristics of this chemical can be adequately described using the TD-B3LYP/6-311++G(d,p) technique. Fig. 1.

Table 2
Calculated λ_{max}, excitation energy first E_{ex}, and oscillator strength (f), of BTPF obtained with different functionals.

Methods	λ_{max}(nm)	E_{ex} (eV)	*f*	MO/ character	(%)
B3LYP/6-31G(d, p)	680.93	1.8195	1.5181	HOMO → LUMO	(99%)
	585.91	2.1146	0.2717	HOMO → LUMO + 1	(93%)
	510.52	2.4269	0.1647	HOMO → LUMO + 2	(94%)
B3LYP/6–31 + G (d,p)	693.93	1.7854	1.5126	HOMO → LUMO	(99%)
	591.53	2.0945	0.3005	HOMO → LUMO + 1	(93%)
	518.92	2.3876	0.1466	HOMO → LUMO + 2	(92%)
B3LYP/6-311G(d, p)	685.68	1.8069	1.5121	HOMO → LUMO	(99%)
	587.66	2.1083	0.2884	HOMO → LUMO + 1	(93%)
	511.51	2.4222	0.1521	HOMO → LUMO + 2	(90%)
B3LYP/6-311++G(d,p)	695.72	1.7809	1.4979	HOMO → LUMO	(99%)
	593.96	2.0859	0.2968	HOMO → LUMO + 1	(93%)
	522.81	2.3698	0.1553	HOMO → LUMO + 2	(94%)
	560.91	2.2088	1.8296	HOMO → LUMO	(81%)
CAM-B3LYP/6-31G(d,p)	463.92	2.6706	0.8157	HOMO → LUMO + 1	(68%)
	386.37	2.2067	0.0430	HOMO → LUMO + 2	(56%)
	652.07	1.9001	1.6230	HOMO → LUMO	(97%)
MPW1PW91/6-31G(d,p)	552.07	2.2442	0.3357	HOMO → LUMO + 1	(96%)
	480.07	2.5808	0.1413	HOMO → LUMO + 2	(92%)

The most dominant transition in electronic transitions is the one with the lowest transition energy and the highest oscillator strength and is followed by a second transition with the lowest oscillator strength. Therefore, the most likely transition between the ground state and the excited state is π-π* or from (HOMO) π to (LUMO) π* transition. The UV–visible absorption spectra of BTPF compound were calculated using various TD-DFT methods and the results were presented in Table 2 (Fig. 2). When looking at the spectra calculated using TD-B3LYP/6-311++G(d,p) method, which gives the λmax value closest to the experimental value, it can be seen that BTPF compound exhibits significant and widespread visible light absorption between 500 and 900 nm and has a large absorption peak at 695.72 nm.

2.3. Geometric optimization

Using the optimized structures of the compound studied, the geometric parameters were determined using the functions listed in Table 3 and presented. Fig. 3 shows the BTPF compound that depicts the placements of bond lengths and dihedral angles.Fig. 4.

It makes sense that single and double bonds between two carbons (C–C and C = C) measure 1.54 Å and 1.34 Å, respectively [44]. Whereas the compound examined had a bond between 1.37 and 1.42 Å long (pictorially demonstrated in Fig. 3), which suggests their improved ability to conjugate and transfer charges. In order to study how the distances between atoms change and how is the overall planarity of the conjugated part affected by the substitutions, a planar structure is more likely to transfer the charge more easily, increasing mobility. In contrast, twists of the rings could hinder the charge transport [45]. The computed bond lengths (d1 and d2) by B3LYP/6 31G(d,p), B3LYP/6-311G(d,p), B3LYP/6-31G+(d,p), and B3LYP/6-311G++(d,p) methods. These values are respectively (1.38, 1.41 Å), (1.38, 1.41 Å), (1.39, 1.41 Å), and (1.38, 1.41 Å). Although the values of the bond lengths (d2; d3) (1.42, 1.38 Å), (1.42, 1.37 Å), (1.42, 1.38 Å), and (1.42, 1.37 Å). The values range between 1.37 Å and 1.42 Å, which demonstrates the character of C = C and the C - C bonds, according to the results obtained. The impact of conjugation can be used to explain this. All of the analyzed dihedral angles θi^{o} range from 180° to 154°, demonstrating a planar confirmation that represents improved conjugation.

From Table 3, it is apparent that the dihedral angles θi^{o} (i = 1–4) values of the studied molecule are very close to 180° for θ1, θ2, and θ3 a result of the presence of atoms that deviate from the fitted plane to a smaller extent, while θ4 which have values between 1554.73°-155.38° as due to intermolecular forces between atoms. The bond lengths di (i = 1–4) are very close to the 1.4 values of the investigated molecule, demonstrating that the molecule exhibits a highly planar structure [46]. This planarity represents improved conjugation that promotes π–π* interaction within the molecule in order to achieve higher mobility of the charge carrier.

2.4. (FMOs) and DOS analysis

Knowing the FMOs of a molecule is important for investigating the optoelectronic capabilities of the molecule by determining the charge density distribution on the molecule. Electrons in a molecule shift from the ground state (HOMO) to the excited state (LUMO) when stimulated

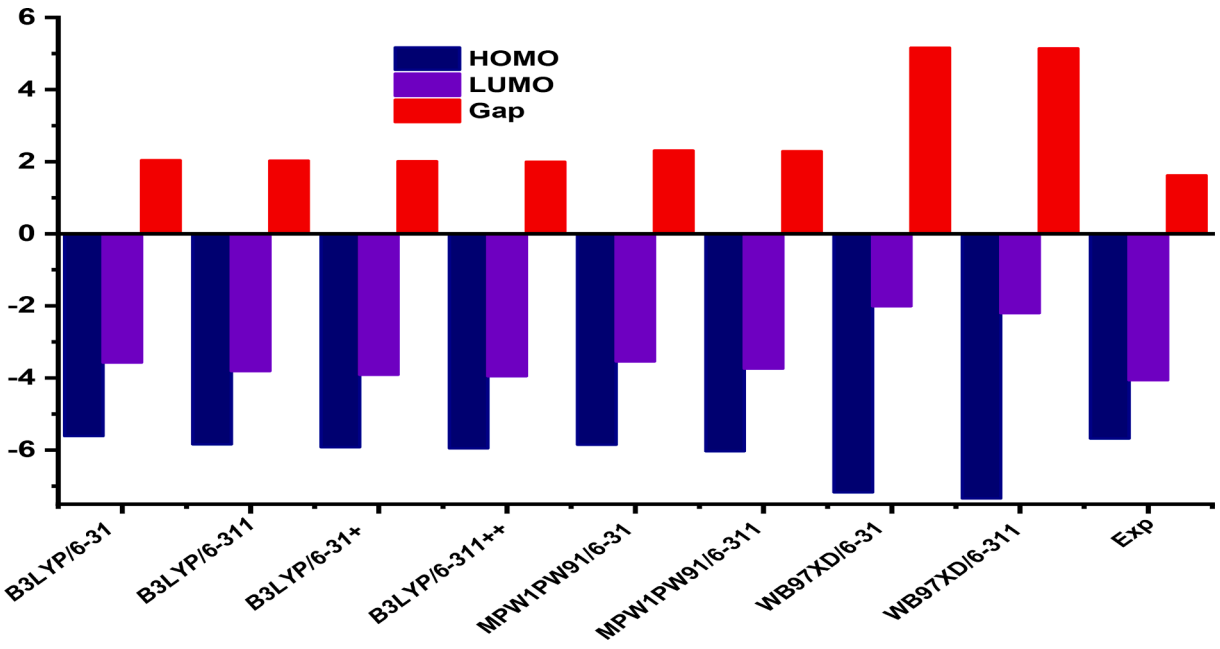

Fig. 1. A comparison of the HOMO, LUMO and band gap energy values of BTPF compound with different methods.

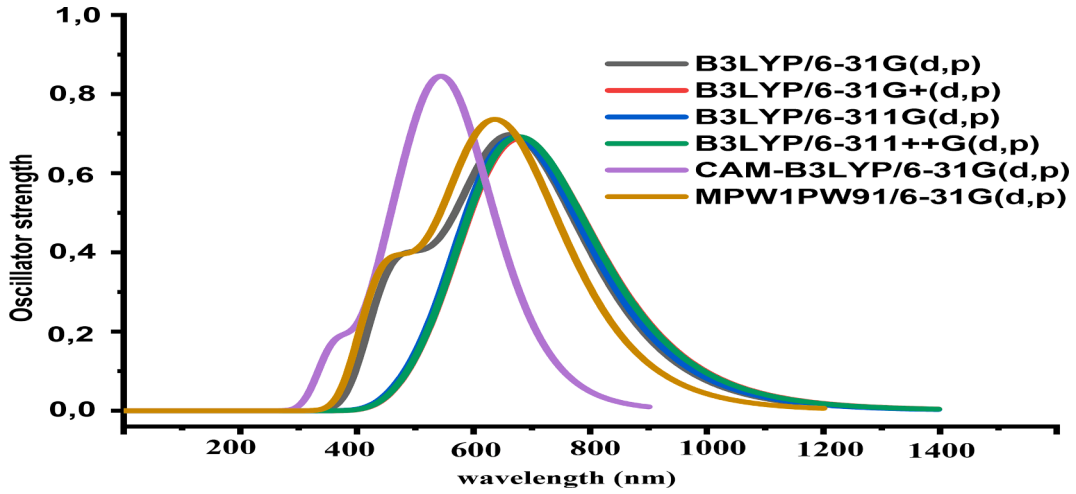

Fig. 2. The UV–Vis absorption spectra of BTPF compound simulated by the TD-DFT with different functionals.

Table 3
Selected distances (Å) and dihedral angle θi(°)of the optimized structure of the BTPF compound obtained at different theoretical levels.

	Bond lengths di(Å)			Dihedral angles θi(°)				
Methods	**d1**	**d2**	**d3**	**d4**	**θ1**	**θ2**	**θ3**	**θ4**
B3LYP/6-31G(d,p)	1.38	1.41	1.42	1.38	−179.66	−179.80	−171.76	−155.33
B3LYP/6-311G(d,p)	1.38	1.41	1.42	1.37	−179.64	−179.73	−169.91	−155.38
B3LYP/6-31G+(d,p)	1.39	1.41	1.42	1.39	−179.79	−179.65	−170.99	−154.73
B3LYP/6-311G++(d,p)	1.38	1.41	1.42	1.37	−179.75	−179.64	−171.04	−154.82

by light of a specific wavelength. The energy difference between these states (HOMO and LUMO) is known as the bandgap (HOMO-LUMO) [47–50]. Fig. 5 shows the HOMO and LUMO shapes of the BTPF molecule. These acceptors cores bonded to the donor compound benzodithiophene group, making the structure acceptor–donor-acceptor (A-D-A) in the studied compound. Due to these electron-withdrawing acceptor groups at the terminal, the charge shift starts from the core of the benzodithiophene donor, it then moves toward the acceptors groups indandiones, resulting in increased delocalization of charge over the BTPF through facilitation in the conjugation. Charge mobility is further aided by the stiff and planner structure of the compound. The charge density in HOMO is concentrated in its benzodithiophene group. The charge density in LUMO is diffused mostly over the indandiones acceptors groups.

It is evident that the benzodithiophene donor group contains the majority of the HOMO distribution, due to their very planar geometry [51]. As opposed to this, the LUMO distribution acceptor (indandione) with lesser spatial overlap improves the electronic coupling between the

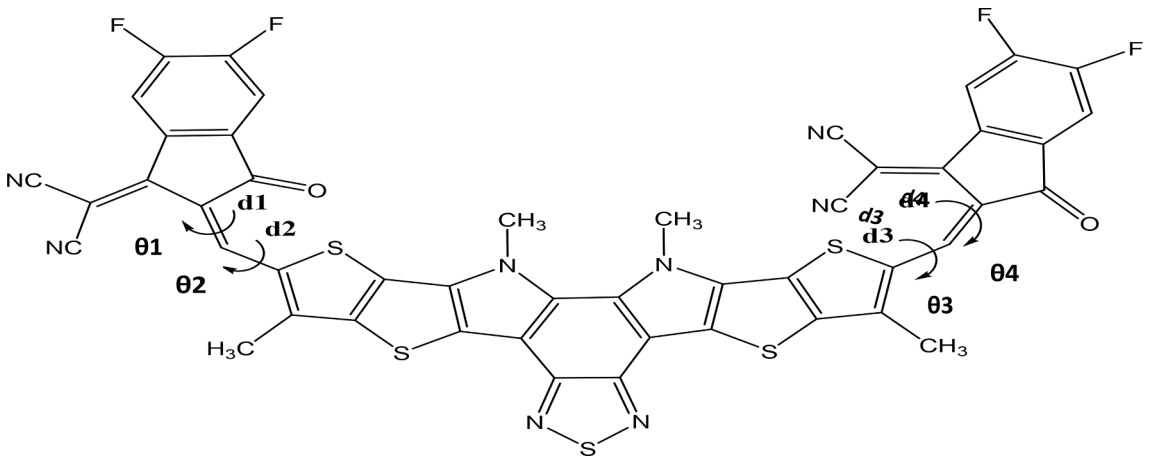

Fig. 3. Bond lengths (di) and dihedral angles (θi) (i = 1–4) of the BTPF compound.

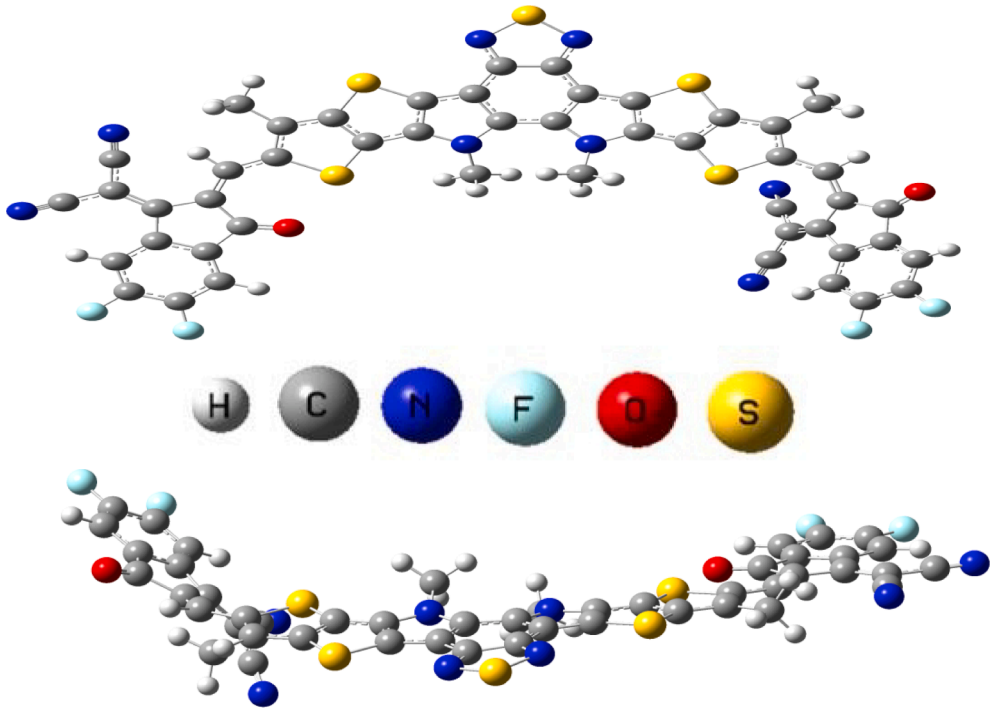

Fig. 4. Optimized structure of the BTPF compound obtained by B3LYP/6–31++G(d,p) level.

acceptor and donor unit, resulting in increased driving force for charge transfer and lower recombination losses. The positive and negative phases are represented by the red and green lobes of FMOs [52]. The results of the spatial delocalization and alignment of the FMO's energy levels suggest that the acceptor exhibits effective charge extraction and transport capabilities, conductivity, and a lower risk of current loss due to recombination. The analyzed molecule charge distribution pattern demonstrates that the recommended molecule has an effective capacity for charge transfer, which is essential for the creation of enhanced OSCs.

For an enhanced demonstration of FMOs, DOS analysis was also performed [53]. DOS is carried out using the B3LYP/6-311++G (d,p) technique. Fig. 6 shows the DOS plots of the compound studied. The attractive electron behavior of end-capped acceptor moieties has affected the distribution array of HOMO and LUMO charge densities, as shown in Fig. 5. According to the findings (Fig. 6), HOMO density is mainly found in the donor benzodithiophene group, while LUMO density is found primarily in the accepting section. The donor entity of the compound studied has the highest HOMO density, whereas the acceptor unit has the lowest empty compound orbital density. As a result of the plots acquired, it was discovered that end-capped acceptors (indandione) efficiently extract electron density, as seen in Fig. 5.

Electrochemical properties were determined using HOMO and LUMO energy values to evaluate BTPF compound as an optoelectronic material, and it was found that BTPF compound is an electron donor. A significant number of molecules were used for this purpose (Fig. 7).

From of the values energies HOMO and LUMO previously calculated by the DFT/B3LYP/6-311++G(d, p) level, we determined several electrochemical parameters, such as chemical hardness, and electronegativity [54] which have successfully been calculated to provide a better understanding of chemical bonding and reactivity in studied systems [55]. Electronegativity (χ) can be defined as the electron donating property of the system and can be identified as the negative of the chemical potential (μ) [56] therefore:

$$\text{Electronegativity}: \chi = -\mu = -(E_{HOMO} + E_{LUMO})/2 \quad (1)$$

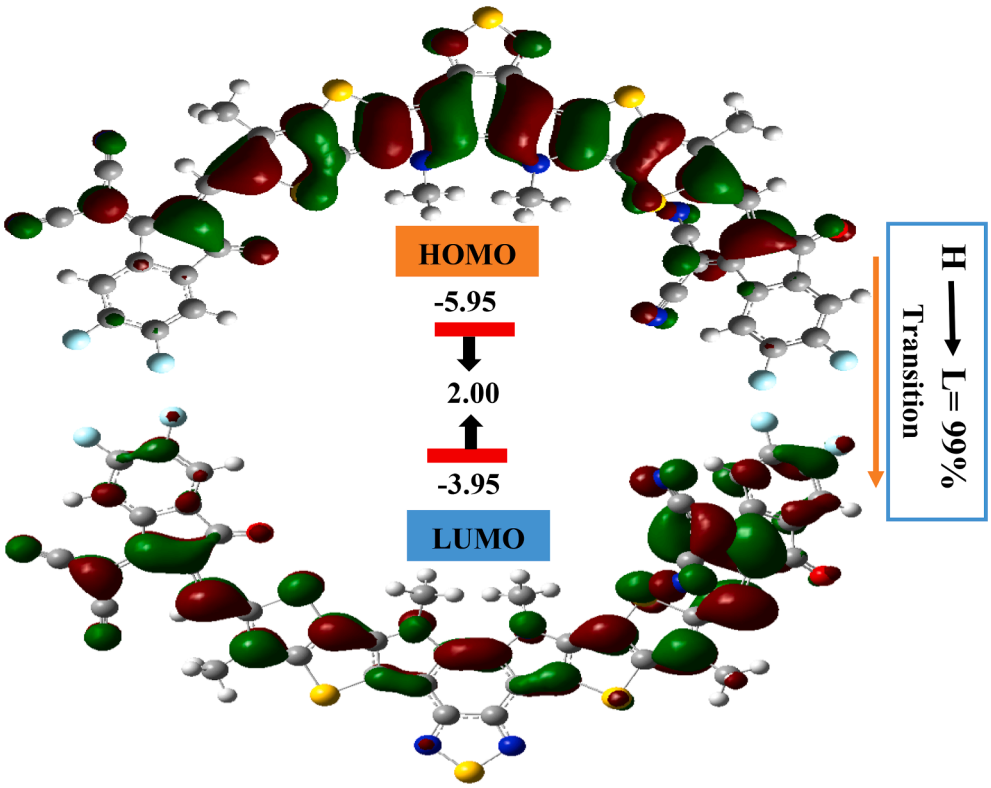

Fig. 5. HOMO and LUMO molecular orbital energy level diagram of the BTPF using B3LYP/6–31++G(d,p) level.

$$\text{Chemical potential}: \mu = (E_{HOMO} + E_{LUMO})/2 \quad (2)$$

The chemical hardness η has been calculated to better understand the resistance of a system to exchange electron density with its environment [57,58].

$$\text{Chemical hardness}: \eta = (E_{LUMO} - E_{HOMO})/2 \quad (3)$$

The chemical hardness and the global electrophilicity index ω of the compound can be calculated using Koopmans theorem as follows:

$$\text{Electrophilicity}: \omega = \mu^2/2\eta \quad (4)$$

Table 4 demonstrates that when compared to the chemical potential BTPF compound (-4.95 eV), the compound PCBM has the lowest chemical potential (-5.10 eV). It demonstrates that the compound studied with the highest chemical potential will transfer electrons to the C_{61} material with the lowest chemical potential. These findings demonstrate that the C_{61} will act as an acceptor material while the BTPF compound acts as a donor material. The compound PCBM has the highest electronegativity (5.10 eV) value when compared to BTPF (4.95 eV), which demonstrates the compound capacity to draw electrons. BTPF will therefore act as an electron donor while the C_{61} compound acts as an electron acceptor in this transfer of electrons. The BTPF compound has the lowest electrophilicity index value (12.25 eV), whereas PCBM has the greatest value of ω (14.45 eV). As a result, more electrophilic than BTPF, demonstrating their capacity to accept electrons. As a result, good electron acceptor. Fig. 8 shows the electronic diagram of the BTPF compound and the acceptor (PCBM).

In this work, we describe a theoretical study of the photovoltaic properties of BTPF compound based on indandione and benzodithiophene units. PCBM has widely been used, due to its high electronic mobility and remarkable electronic conductivity [59–61]:

The power conversion efficiency η was calculated according to the following expression (5) [62].

$$\eta = \frac{P_{max}}{P_{in}} = \frac{FF \times V_{OC} \times J_{SC}}{P_{in}} \quad (5)$$

Where P_{max} is the greatest amount of power that the cell is capable of producing, P_{in} stands for incident power density, J_{sc} for short-circuit current density, Voc for open-circuit voltage, and FF for fill factor. The energy difference between the HOMO and LUMO is known as the maximum open circuit voltage (Voc) of a solar cell. The research team of Brabec and Scharber [63,64]demonstrated in particular that the following relation may be used to predict the Voc of a donor/acceptor couple:

$$Voc = \frac{1}{e}(|E^{D}_{HOMO}| - |E^{A}_{LUMO}|) - 0.3 \quad (6)$$

According to the previous equation, the open circuit voltage V_{OC} linearly depends on the HOMO level of the donor and the LUMO level of the acceptor [65]. From Fig. 8, the theoretical value of the open circuit voltage Voc equals 1.45 V. This value is sufficient for a better injectionof efficient electrons. Therefore, the compound studied can be suggested as asensitizer, since the process of injecting electrons from the excited moleculeto the conduction band of PCBM will be spontaneous.

2.5. Transition density matrix (TDM), and reduced density gradient (RDG)

Most Frenkel excitons (bonded electron-hole pairs) are held together by a strong Coulomb force during photoexcitation rather than splitting into free charge carriers. It also happens with efficient exciton dissociation of free charge carriers to improve Jsc and FF performance. TDM calculations were performed using TD/B3LYP/6-311++G(d,p) to learn more about electronic excitation mechanisms, electron hole localization, and consistency of particular excitations between segments of the molecular skeleton studied. Therefore, three parts of the studied molecule were separated and labeled as A for acceptor units and D for central core unit (benzodithiophene). The bottom and left sides of the matrix (as

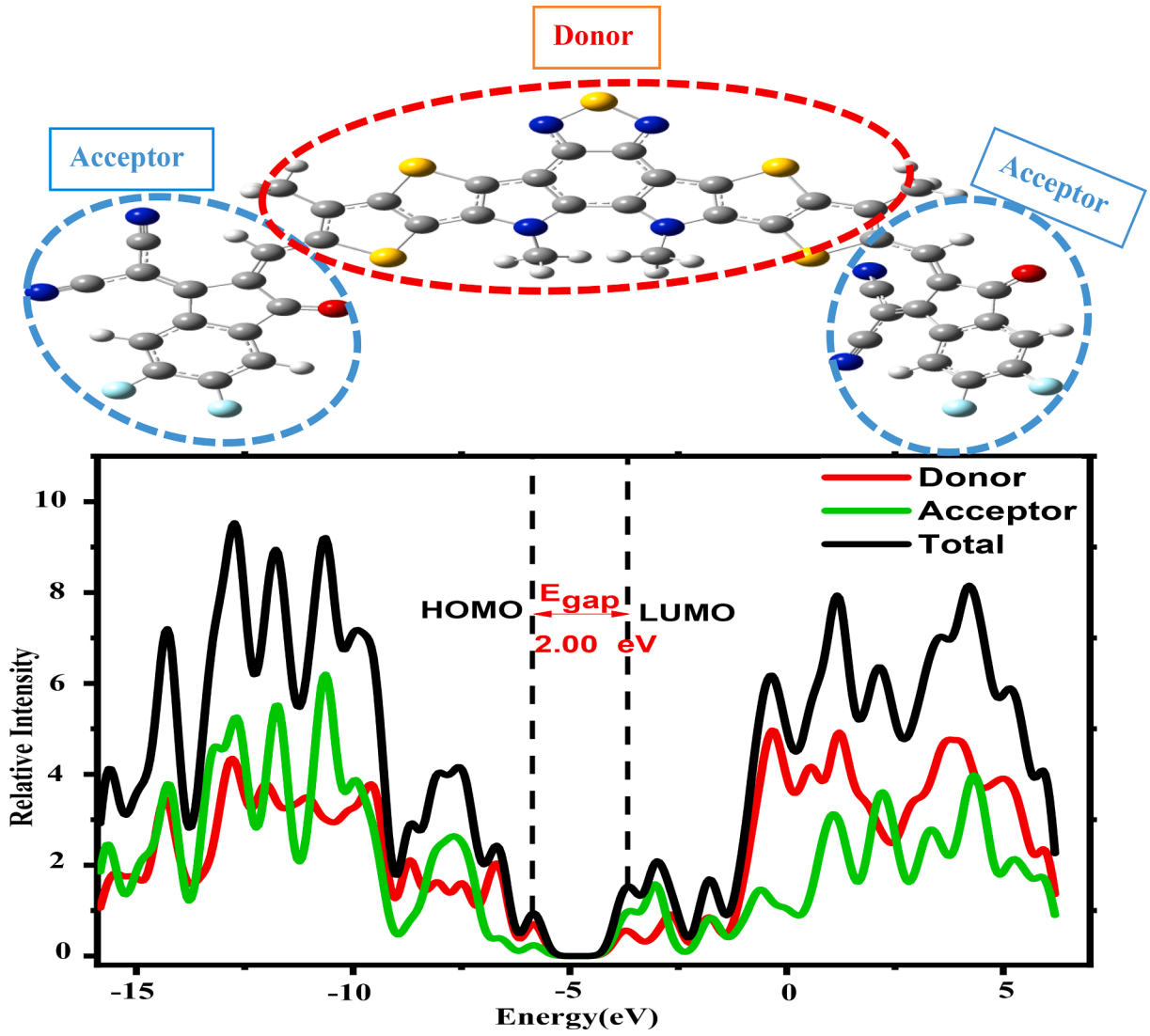

Fig. 6. Density of state (DOS) plots of the BTPF at B3LYP/6-311++G (d,p) level.

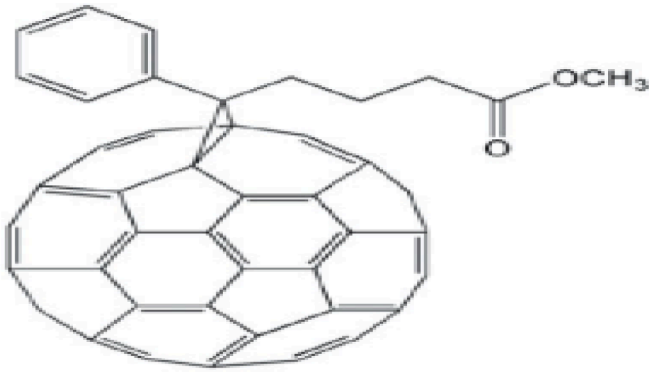

Fig. 7. Molecular structure of phenyl-C61-butyric acid methyl ester (PCBM) acceptor.

illustrated in Fig. 9) specify the number of atoms in the examined molecule, and the right y-axis of the matrix indicates the electron density coefficient.

The TDM maps diagonal terms can show which atoms have substantial distributions of both the hole and the electron at the same time. In order to reinforce these results obtained with TDM, we compared the

Table.4
Electronic and chemical parameters (HOMO, LUMO (eV)), chemical hardness (η), chemical potential (μ), electronegativity (χ), and dipole moment (ρ) obtained by B3LYP/6-311++G(d, p) of the compound studied.

Compound	E_{HOMO}	E_{LUMO}	μ (eV)	η (eV)	χ (eV)	ω (eV)
BTPF	−5.95	−3.95	−4.95	1.00	4.95	12.25
PCBM	−6.00	−4.20	−5.10	0.90	5.10	14.45

TDM maps findings to *iso*-surface density maps and an RDG Fig. 10 color-coded map in order to comprehend them better.

According to Fig. 9, based on the colors in the TDM map, the central BTPF core (benzodithiophene) was found to have a hole distributed along the diagonal, whereas the acceptors (A) were found to have an electron distributed along the diagonal. These results are in line with what the *iso*-surface density maps show to be the scenario. This indicates that the electron density is constantly switching from the donor core to the acceptor fragments of indandione.

The color-coded RDG map shows strong interactions due to hydrogen bonding (blue color), greater interactions due to steric effect (red color), and intermediate Van der Waals interactions (the green color) [66]. The blue and green sections of the RDG (Fig. 10 b)) are indicative of an increase in the amount of hydrogen bonds and van der Waals interaction

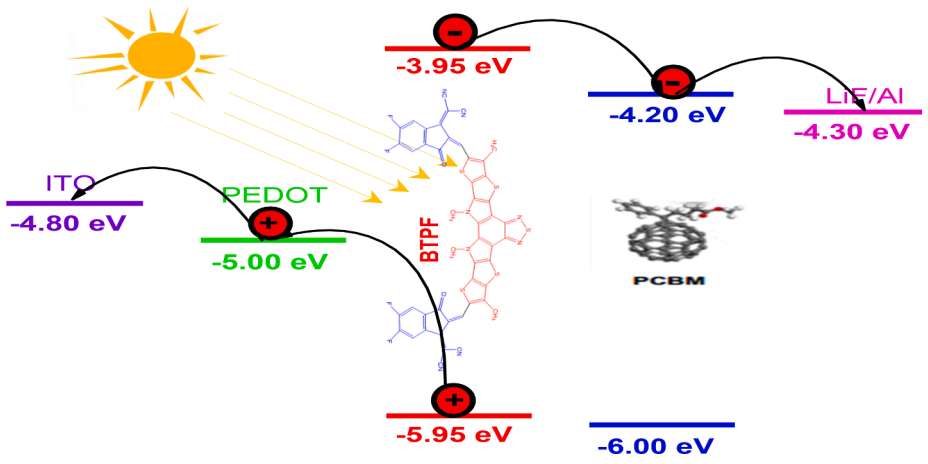

Fig. 8. Electronic diagram of BTPF compound and PCBM acceptor.

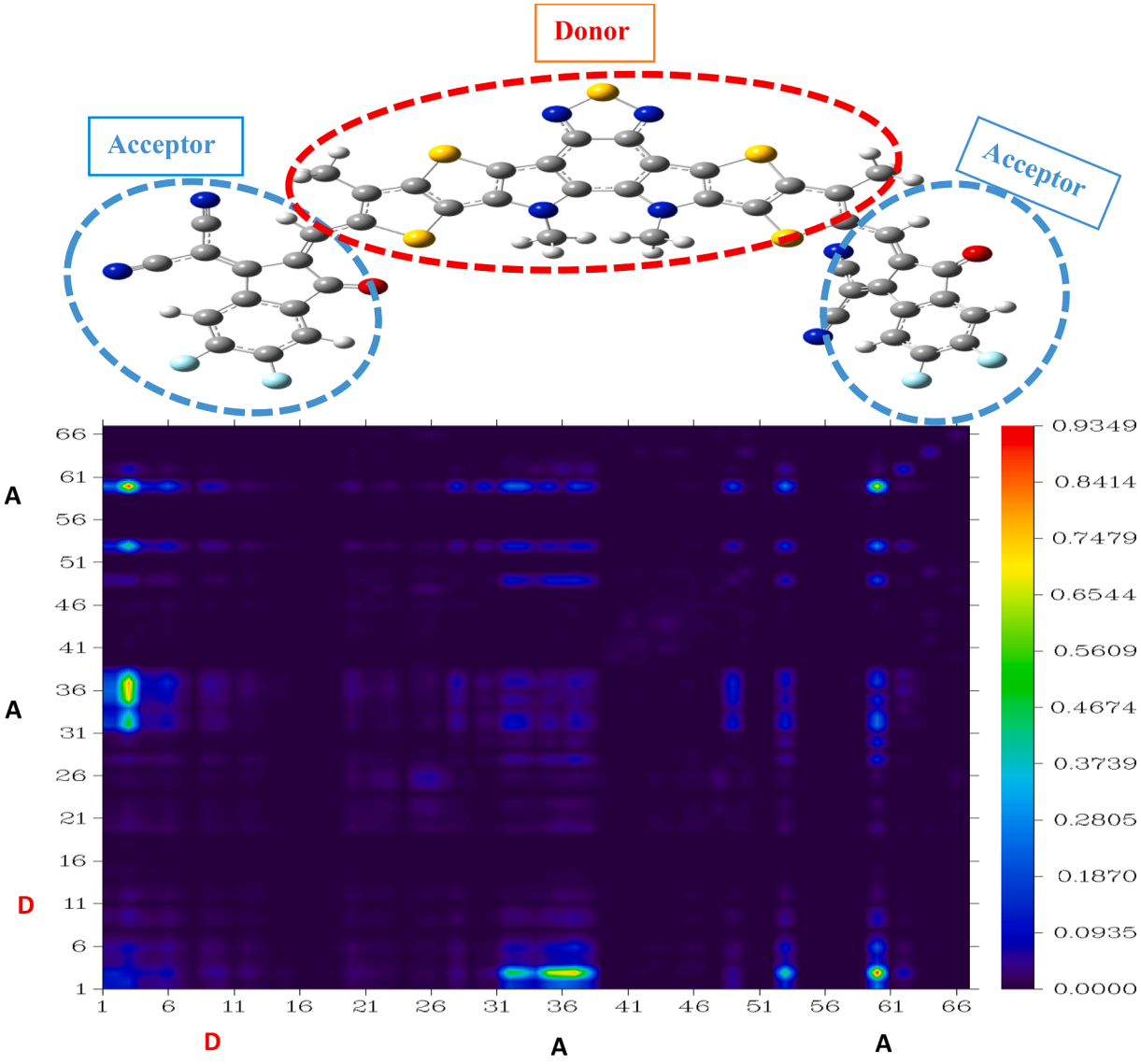

Fig. 9. TDM plots of the BTPF at B3LYP/6-311++G(d,p) level.

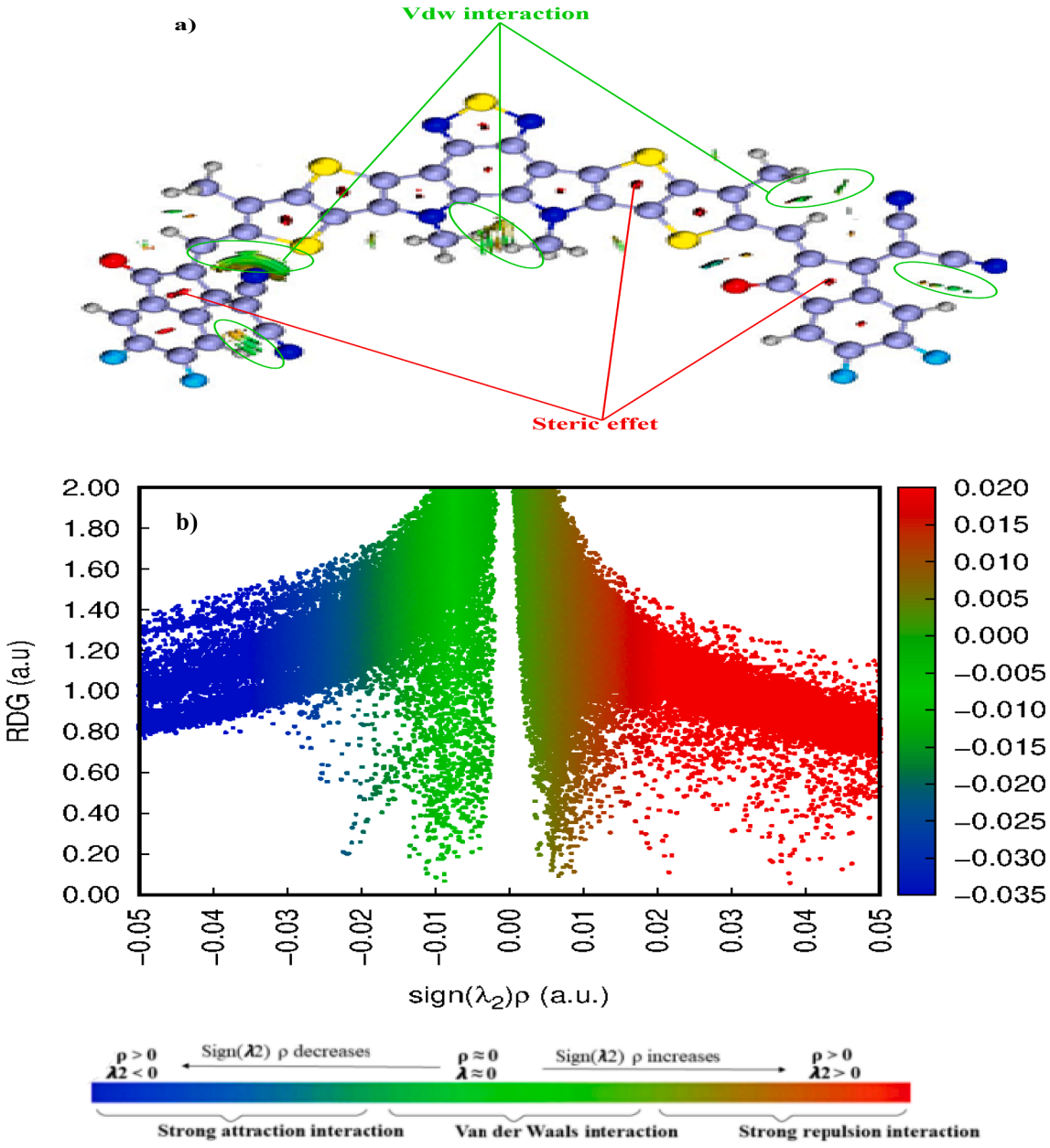

Fig. 10. The plot of the reduced density gradient (RDG) a) 3D isosurface density maps and b) scatter diagram.

regions, as seen in (Fig. 10 a)) (the scatter diagram). The interaction strength can be accurately determined using the low gradient peak densities (RDG). Plotting ρ(r) versus sign λ2 helps one understand the type and strength of interactions, it is preferable to utilize the sign λ2 to distinguish between bonding (λ2 < 0) and nonbonding (λ2 > 0) interactions when the 3D maps RDG values are versus [67–69].

3. Conclusion

In this study, the structural, optical and electronic properties of BTPF compound were theoretically calculated using different functionals of the Density Functional Theory (DFT) method. This molecule was synthesized by L. Hong and these collaborators used it as acceptor material. The first objective of this study is to find the appropriate DFT and TD-DFT functional that reflects the experimental results obtained. On the other hand, it was to test the compound as electron donor with different fullerene derivatives as acceptor. With the results obtained, it was found that the DFT/ B3LYP/6-311++G(d,p) level gave very good results to predict the electrical and optical properties of the molecule. The BTPF compound was calculated to have a gap energy of 2.00 eV at the B3LYP/ 6-311++G(d,p) level and diffuse visible light absorption between 500 and 900 nm and a large absorption peak at 695.72 nm in its isolated state. The calculated Voc values for the studied compound with PCBM as acceptor are 1.45 V. This value is sufficient for possible efficient electron injection from BTPF as a donor to the conduction band of the PC61BM. Based on many criteria, BTPF compound can be proposed as a promising candidate in OSCs as a blended electron donor with PCBM fullerene as acceptor.

Declaration of Competing Interest

The authors declare that they have no known competing financial interests or personal relationships that could have appeared to influence the work reported in this paper.

Data availability

No data was used for the research described in the article.

References

[1] M.R.S.A. Janjua, Deciphering the role of invited guest bridges in non-fullerene acceptor materials for high performance organic solar cells, Synth. Met. 279 (2021), 116865, https://doi.org/10.1016/j.synthmet.2021.116865.

[2] M.R.S.A. Janjua, All-small-molecule organic solar cells with high fill factor and enhanced open-circuit voltage with 18.25 % PCE: physical insights from quantum chemical calculations, Spectrochim. Acta – Part A Mol. Biomol. Spectrosc. 279 (2022), 121487, https://doi.org/10.1016/j.saa.2022.121487.

[3] M.R.S.A. Janjua, Quantum chemical design of D–π–A-type donor materials for highly efficient, photostable, and vacuum-processed organic solar cells, Energy Technol. 9 (10) (2021), 2100489.

[4] A. Mahmood, J. Yang, J. Hu, X. Wang, A. Tang, Y. Geng, Q. Zeng, E. Zhou, Introducing four 1,1-dicyanomethylene-3-indanone end-capped groups as an alternative strategy for the design of small-molecular nonfullerene acceptors, J. Phys. Chem. C 122 (51) (2018) 29122–29128.

[5] M.R.S.A. Janjua, How does bridging core modification alter the photovoltaic characteristics of triphenylamine-based hole transport materials? Theoretical understanding and prediction, Chem. - A Eur. J. 27 (2021) 4197–4210, https://doi.org/10.1002/chem.202004299.

[6] Y. Cui, Y.e. Xu, H. Yao, P. Bi, L. Hong, J. Zhang, Y. Zu, T. Zhang, J. Qin, J. Ren, Z. Chen, C. He, X. Hao, Z. Wei, J. Hou, Single-junction organic photovoltaic cell with 19% efficiency, Adv. Mater. 33 (41) (2021) 2102420.

[7] L. Zhu, M. Zhang, J. Xu, C. Li, J. Yan, G. Zhou, W. Zhong, T. Hao, J. Song, X. Xue, Z. Zhou, R. Zeng, H. Zhu, C.-C. Chen, R.C.I. MacKenzie, Y. Zou, J. Nelson, Y. Zhang, Y. Sun, F. Liu, Single-junction organic solar cells with over 19% efficiency enabled by a refined double-fibril network morphology, Nat. Mater. 21 (6) (2022) 656–663.

[8] H. Yao, L. Ye, H. Zhang, S. Li, S. Zhang, J. Hou, Molecular design of benzodithiophene-based organic photovoltaic materials, Chem. Rev. 116 (12) (2016) 7397–7457.

[9] K. Atiq, M. Adnan, S. Muhammad, R. Hussain, Z. Irshad, M.U. Khan, Fused ring pyrrolo [3, 2-b] pyrrole-based tilde-shaped acceptor molecules for highly efficient organic solar cells, J. Phys. Chem. Solid 176 (2023) 111228.

[10] S. Alam, M. Shaheer Akhtar, H.-S. Shin, S. Ameen, New energetic indandione based planar donor for stable and efficient organic solar cells, Sol. Energy 201 (2020) 649–657.

[11] Q.A. Khoirun Nisa, D.H. Son, J.H. Kim, A step-by-step strategy to enhancing the photovoltaic performance of indandione-based polymers, Dye Pigment 207 (2022) 110760.

[12] J. Wang, X. Zhan, Fused-ring electron acceptors for photovoltaics and beyond, Acc. Chem. Res. 54 (1) (2021) 132–143.

[13] M. Haroon, M.R.S.A. Janjua, Exploring the effect of end-capped modifications of carbazole-based fullerene-free acceptor molecules for high-performance indoor organic solar cell applications, J. Comput. Electron. 21 (1) (2022) 40–51.

[14] A. Mahmood, J.-L. Wang, A time and resource efficient machine learning assisted design of non-fullerene small molecule acceptors for P3HT-based organic solar cells and green solvent selection, J. Mater. Chem. A 9 (28) (2021) 15684–15695.

[15] M.R.S.A. Janjua, Theoretical understanding and role of guest π-bridges in triphenylamine-based donor materials for high-performance solar cells, Energy Fuel 35 (15) (2021) 12451–12460.

[16] M. Waqas, N.M.A. Hadia, M.M. Hessien, J. Iqbal, G.A.M. Mersal, S. Hameed, A. M. Shawky, Z. Aloui, M.A.A. Ibrahim, R. Ahmad Khera, End-group Modification of terminal acceptors on benzothiadiazole-based BT2F-IC4F molecule to establish efficient organic solar cells, J. Mol. Liq. 368 (2022), 120770, https://doi.org/10.1016/j.molliq.2022.120770.

[17] F. Abbas, M.D. Mohammadi, H. Louis, E.C. Agwamba, High-performance non-fullerene acceptor-analogues designed from dithienothiophen [3,2-b]-pyrrolobenzothiadiazole (TPBT) donor materials, J. Mol. Model. 29 (2023) 31, https://doi.org/10.1007/s00894-022-05435-x.

[18] S.S. Alarfaji, D. Fatima, B. Ali, A. Sattar, R. Hussain, R. Hussain, K. Ayub, Computational investigation of near-infrared-absorbing indeno[1,2- b]indole analogues as acceptors in organic photovoltaic devices, ACS Omega 8 (1) (2023) 1430–1442.

[19] M.I. Khan, N.M.A. Hadia, A.M. Shawky, M.M. Hessien, M. Essid, S.J. Akram, J. Iqbal, N.S. Alatawi, G.A.M. Mersal, R.A. Khera, Quantum mechanical modeling of fused rings-based small-donor molecules with enhanced optoelectronic attributes for high performance organic photovoltaic cells, J. Phys. Chem. Solid 174 (2023), 111140, https://doi.org/10.1016/j.jpcs.2022.111140.

[20] M. Khalid, M. Khan, K. Mahmood, M. Arshad, M. Imran, A.A.C. Braga, et al., Theoretical designing of non-fullerene derived organic heterocyclic compounds with enhanced nonlinear optical amplitude: a DFT based prediction, Sci. Rep. 12 (2022) 1–14, https://doi.org/10.1038/s41598-022-21894-x.

[21] L. Hong, H. Yao, Z. Wu, Y. Cui, T. Zhang, Y.e. Xu, R. Yu, Q. Liao, B. Gao, K. Xian, H. Y. Woo, Z. Ge, J. Hou, Eco-compatible solvent-processed organic photovoltaic cells with over 16% efficiency, Adv. Mater. 31 (39) (2019) 1903441.

[22] X. Liu, L. Gu, Q. Zhang, J. Wu, Y. Long, Z. Fan, All-printable band-edge modulated ZnO nanowire photodetectors with ultra-high detectivity, Nat. Commun. 5 (2014) 4007.

[23] A. Frisch, Gaussian 09W Reference. Wallingford, USA, 25p, 2009; 470.

[24] R. Dennington, T.A. Keith, J.M. Millam, GaussView, version 6.0. 16. Semichem Inc Shawnee Mission KS, 2016.

[25] J.P. Finley, Using the local density approximation and the LYP, BLYP and B3LYP functionals within reference-state one-particle density-matrix theory, Mol. Phys. 102 (7) (2004) 627–639.

[26] J.-D. Chai, M. Head-Gordon, Long-range corrected hybrid density functionals with damped atom–atom dispersion corrections, PCCP 10 (2008) 6615–6620.

[27] C. Adamo, V. Barone, Exchange functionals with improved long-range behavior and adiabatic connection methods without adjustable parameters: the mPW and mPW1PW models, J. Chem. Phys. 108 (2) (1998) 664–675.

[28] M.T.P. Beerepoot, D.H. Friese, N.H. List, J. Kongsted, K. Ruud, Benchmarking two-photon absorption cross sections: performance of CC2 and CAM-B3LYP, PCCP 17 (29) (2015) 19306–19314.

[29] A. Azaid, T. Abram, R. Kacimi, A. Sbai, T. lakhlifi, M. Bouachrine, Organic materials based with D– π –A structure based on thiophene and anthracene for application in dye-sensitized solar cells, Mater. Today:. Proc. 45 (2021) 7363–7369.

[30] M. Bouachrine, T. Abram, R. Kacimi, L. Bejjit, B.M. Nassiri, New organic materials based on thiophene for photovoltaic device: theoretical investigation, Turkish Comput Theor Chem 2 (2018) 36–48. https://doi.org/10.33435/tcandtc.410314.

[31] R. Kacimi, T. Abram, L. Bejjit, M. Bouachrine, New organic materiel based on benzothiadiazole for photovoltaic application solar cells, Mater. Today:. Proc. 13 (2019) 1188–1196.

[32] R. Kacimi, T. Abram, W. Saidi, L. Bejjit, M. Bouachrine, New organic molecular based on Bis-Dipolar Diphenylamino-EndcappedOligo Aryl Fluorene Application for organic solar cells, Mater. Today:. Proc. 13 (2019) 1178–1187, https://doi.org/10.1016/j.matpr.2019.04.086.

[33] R. Kacimi, T. Abram, L. Bejjit, M. Bouachrine, Compounds derived from flavonoids for photovoltaic applications. computational chemical investigations, J Turkish Chem Soc Sect A Chem 5 (2018) 1009–1020. https://doi.org/10.18596/jotcsa.420458.

[34] C. Lee, W. Yang, R.G. Parr, Development of the Colle-Salvetti correlation-energy formula into a functional of the electron density, Phys. Rev. B 37 (2) (1988) 785–789.

[35] A.D. Becke, Density-functional thermochemistry. I. The effect of the exchange-only gradient correction, J. Chem. Phys. 96 (1992) 2155–2160.

[36] A. Azaid, T. Abram, M. Alaqarbeh, M. Raftani, R. Kacimi, A. Sbai, et al., Design new organic material based on triphenylamine (TPA) with D- π -A- π -D structure used as an electron donor for organic solar cells : A DFT approach, J. Mol. Graph. Model. 122 (2023), 108470, https://doi.org/10.1016/j.jmgm.2023.108470.

[37] R.a.G.E. Scuseriaa, An efficient implementation of time-dependent density-functional theory for the calculation of excitation energies of large molecules, J. Chem. Phys. 19 (1998) 8218–8224.

[38] C. Bannwarth, S. Grimme, A simplified time-dependent density functional theory approach for electronic ultraviolet and circular dichroism spectra of very large molecules, Comput. Theor. Chem. 1040 (2014) 45–53.

[39] M. Bourass, A.T. Benjelloun, M. Benzakour, M. Mcharfi, M. Hamidi, S.M. Bouzzine, et al., Theoretical Studies by Using the DFT and TD-DFT of the effect of the bridge formed of thienopyrazine in solar cells, J Mater Environ Sci 6 (2015) 1542–1553.

[40] N.M. O'boyle, A.L. Tenderholt, K.M. Langner, Cclib: a library for package-independent computational chemistry algorithms, J. Comput. Chem. 29 (5) (2008) 839–845.

[41] T. Lu, F. Chen, Multiwfn: a multifunctional wavefunction analyzer, J. Comput. Chem. 33 (5) (2012) 580–592.

[42] W. Humphrey, A. Dalke, K. Schulten, VMD: visual molecular dynamics, J. Mol. Graph. 14 (1) (1996) 33–38.

[43] R. Kacimi, M. Raftani, T. Abram, A. Azaid, H. Ziyat, L. Bejjit, M.N. Bennani, M. Bouachrine, Heliyon Theoretical design of D- π -A system new dyes candidate for DSSC application, Heliyon 7 (6) (2021), e07171, https://doi.org/10.1016/j.heliyon.2021.e07171.

[44] W.-Q. Sun, J.-B. Hu, Y.-J. Jiang, N. Xu, L.-Y. Wang, J.-H. Li, Y.-Q. Hu, S. Duttwyler, Y.-B. Zhang, Flexible molecular sieving of C2H2 from CO2 by a new cost-effective metal organic framework with intrinsic hydrogen bonds, Chem. Eng. J. 439 (2022), 135745, https://doi.org/10.1016/j.cej.2022.135745.

[45] A. Azaid, M. Raftani, M. Alaqarbeh, R. Kacimi, New organic dye-sensitized solar cells based on the D – A – p – A structure for efficient DSSCs: DFT / TD- DFT investigations, RCA Adv. (2022) 30626–30638, https://doi.org/10.1039/d2ra05297k.

[46] O. Ninis, R. Kacimi, H. Bouaamlat, M. Abarkan, M. Bouachrine, Theoretical studies of photovoltaic properties for design of new Azo-Pyrrole photo-sensitizer materials as dyes in solar cells, J Mater Environ Sci 8 (2017) 2572–2578.

[47] R. Kacimi, T. Abram, M. Bourass, L. Bejjit, K. Alimi, M. Bouachrine, Molecular design of D-A–D conjugated molecules based on fluorene for organic solar cells. Opt, Quantum Electron. 51 (2019), https://doi.org/10.1007/s11082-019-1799-7.

[48] R. Kacimi, J. Iqbal, L. Louazri, A. Alioui, M. Hamidi, L. Bejjit, M.N. Bennani, M. Bouachrine, Drafting novel N-phenylnaphthalen-1-amine-based dyes for designing highly proficient organic solar cells: theoretical investigation of the π-linker influence on photovoltaic properties, Opt. Quantum Electron. 54 (2) (2022), https://doi.org/10.1007/s11082-021-03503-9.

[49] R. Kacimi, M. Bourass, T. Toupance, N. Wazzan, M. Chemek, A. El Alamy, L. Bejjit, K. Alimi, M. Bouachrine, Computational design of new organic (D–π–A) dyes based on benzothiadiazole for photovoltaic applications, especially dye-sensitized solar cells, Res. Chem. Intermed. 46 (6) (2020) 3247–3262.

[50] R. Kacimi, M. Chemek, A. Azaid, M.N. Bennani, K. Alimi, L. Bejjit, Organic materials based on thiophene and benzothiadiazole for organic solar cells,

Computational investigations 5 (2020) 1–11. https://doi.org/10.23647/ca.md20202804.
[51] S.J. Akram, N.M.A. Hadia, J. Iqbal, R.F. Mehmood, S. Iqbal, A.M. Shawky, A. Asif, H.H. Somaily, M. Raheel, R.A. Khera, Impact of various heterocyclic π-linkers and their substitution position on the opto-electronic attributes of the A–π–D–π–A type IECIO-4F molecule: a comparative analysis, RSC Adv. 12 (32) (2022) 20792–20806.
[52] R.N. Aljawfi, S.M. Sherif, S. Akef, M.J. Alam, A.A. Ahmed, M.A. Swillam, Photon harvesting and light trapping in pentacene and PTCDI-C13H27 for organic solar cell application, Optik (Stuttg) 258 (2022), 168931.
[53] A. Azaid, R. Kacimi, M. Alaqarbeh, M. Raftani, T. Abram, A. Sbai, et al., Design of a D-Di–π–A architecture with different auxiliary donors for dye-sensitized solar cells: density functional theory/time-dependent-density functional theory study of the effect of secondary donors, Adv Theory Simulations 2300054 (2023) 1–14, https://doi.org/10.1002/adts.202300054.
[54] R. Kacimi, M. Chemek, A. Bouchikhi, H. Lgaz, A. Azaid, M. Raftani, M. Naciri Bennani, H.-S. Lee, K. Alimi, L. Bejjit, M. Bouachrine, Synthesis, experimental and theoretical characterization of a new copolymer bearing pyrrole and anthracene units, J. Photochem. Photobiol. A Chem. 432 (2022), 114056, https://doi.org/10.1016/j.jphotochem.2022.114056.
[55] M. Khalid, Z. Saeed, I. Shafiq, M.A. Asghar, A.A.C. Braga, S.M. Alshehri, M. S. Akram, S.C. Ojha, Designing strategies towards non-fullerene DTCR1 based compounds for the exploration of non-linear optical behavior, J. Saudi Chem. Soc. 27 (4) (2023) 101683, https://doi.org/10.1016/j.jscs.2023.101683.
[56] R.S. Mulliken, Electronic structures of molecules XI. Electroaffinity, molecular orbitals and dipole moments, J. Chem. Phys. 3 (9) (1935) 573–585.
[57] Z. Zhou, R.G. Parr, J.F. Garst, Tetrahedron Left. 29 (1988) 4843-4846; Z. Zhou, R. G. Parr, J. Am. Chem. Soc. 111 (1989) 7371–7379.
[58] R.G. Parr, L.V. Szentpály, S. Liu, Electrophilicity index, J. Am. Chem. Soc. 121 (1999) 1922–1924.
[59] S. Lalik, S. Urban, J. Świergiel, K. Bogdanowicz, A. Iwan, M. Marzec, Influence of the (E)-N-(4-diphenylamino)benzylidene)benzo[d]thiazol-2-imine on the dielectric properties of P3HT, PCBM and P3HT:PCBM system in a wide temperature and frequency range, Mater. Sci. Eng. B Solid-State Mater. Adv. Technol. (2023) 287, https://doi.org/10.1016/j.mseb.2022.116161.
[60] J. Li, K. Zhuang, Y. Mao, C. Liu, M. Pang, H. Li, Nanoarchitectonics of mesoporous carbon from C60/PCBM hybrid crystals for supercapacitor, Carbon N Y 201 (2023) 449–459, https://doi.org/10.1016/j.carbon.2022.09.051.
[61] A.A. El, M. Bourass, A. Amine, R. Kcimi, M. Bouachrine, New small compounds based on thienylenevinylene with D-A-D structure for bhj applications: Theoretical study, Orbital 12 (2020) 220–231. https://doi.org/10.17807/orbital.v12i4.1524.
[62] A. Gadisa, M. Svensson, M.R. Andersson, O. Inganäs, Correlation between oxidation potential and open-circuit voltage of composite solar cells based on blends of polythiophenes/fullerene derivative, Appl. Phys. Lett. 84 (2004) 1609–1611.
[63] M.C. Scharber, D. Mühlbacher, M. Koppe, P. Denk, C. Waldauf, A.J. Heeger, et al., Design rules for donors in bulk-heterojunction solar cells—towards 10% energy-conversion efficiency, Adv. Mater. 18 (2006) 789–794.
[64] G. Dennler, M.C. Scharber, T. Ameri, P. Denk, K. Forberich, C. Waldauf, et al., Design rules for donors in bulk-heterojunction tandem solar cells towards 15% energy-conversion efficiency, Adv. Mater. 20 (2008) 579–583.
[65] D. Nebbach, F. Agda, S. Kaya, F. Siddique, T. Lakhlifi, M. Aziz Ajana, et al., Non-fullerene acceptor IDIC based on indacinodithiophene used as an electron donor for organic solar cells: a computational study, J. Mol. Liq. 348 (2022), 118289, https://doi.org/10.1016/j.molliq.2021.118289.
[66] S. Chebil, M. Chemek, T. Mestiri, K. Alimi, Theoretical enhancement of the electronic and optical properties of a new D-π-A-π-D synthesized donor molecule for a new generation of fullerene-based bulk heterojunction (BHJ) for new organic solar cells devices, J. Mol. Graph. Model. 115 (2022), 108226, https://doi.org/10.1016/j.jmgm.2022.108226.
[67] A.S. Kazachenko, N. Issaoui, M. Medimagh, O. Fetisova, Y.D. Berezhnaya, E. V. Elsufev, et al., Experimental and theoretical study of the sulfamic acid-urea deep eutectic solvent, J. Mol. Liq. 363 (2022), 119859, https://doi.org/10.1016/j.molliq.2022.119859.
[68] A.S. Kazachenko, N. Issaoui, A. Sagaama, Y.N. Malyar, O. Al-Dossary, L. G. Bousiakou, et al., Hydrogen bonds interactions in biuret-water clusters: FTIR, X-ray diffraction, AIM, DFT, RDG, ELF, NLO analysis, J. King Saud. Univ. – Sci. 34 (2022), 102350, https://doi.org/10.1016/j.jksus.2022.102350.
[69] U. Sohail, F. Ullah, T. Mahmood, K. Ayub, Olympicene as a high-performance sensor for lung irritants: a dispersion corrected DFT insight, Mater. Sci. Semicond. Process. 144 (2022), 106620, https://doi.org/10.1016/j.mssp.2022.106620.